PRAMANA
— journal of
physics

Vol. 77, No. 2
August 2011
pp. 345–355

Experimental investigation of ultrasonic velocity anisotropy in magnetic fluids: Influence of grain–grain interaction

KRUTI SHAH and R V UPADHYAY*

P.D. Patel Institute of Applied Sciences and K.C. Patel R & D Center,
Charotar University of Science & Technology, Education Campus, Changa 388 421, India
*Corresponding author. E-mail: rvu.as@ecchanga.ac.in

MS received 11 October 2010; revised 13 January 2011; accepted 14 February 2011

Abstract. Magnetic field-induced dispersion of ultrasonic velocity in a $Mn_{0.7}Zn_{0.3}Fe_2O_4$ fluid (applied magnetic field is perpendicular to the ultrasonic propagation vector) is determined by employing continuous wave method. The magnitude of dispersion initially decreases with increasing field, then increases and reaches a plateau at higher fields. Results indicate that the velocity anisotropy is dominated by grain–grain interactions rather than grain–field interaction. At the critical temperature, the grain–grain interaction becomes weak as the transverse component of the particle/cluster moment is larger than the longitudinal one and the system reaches saturation even at low field. These observed variations in the field-induced anisotropy are analysed by incorporating the moment distribution of particles in Tarapov's theory (*J. Magn. Magn. Mater.* **39**, 51 (1983)).

Keywords. Magnetic fluids; ultrasonic wave; sound velocity; anisotropy.

PACS Nos 47.65.Cb; 47.35.Rs; 47.57.J-; 62.60.+v

1. Introduction

A magnetic fluid is a colloidal dispersion of ferro- or superparamagnetic nanoparticles in a carrier liquid. The properties of the fluid are isotropic in the absence of magnetic field but the liquid undergoes restructuring under external magnetic field. This field-induced anisotropy is manifested in several physical properties of the fluid, like viscosity, which gives rise to novel properties as elasticity and yield stress [1–4]. Hence, experimental investigations of field-induced anisotropy are useful to characterize the physical state of a fluid. But, because the magnetic fluids are opaque, it is difficult to analyse them by optical methods. Experimental and theoretical studies of ultrasonic wave propagation in magnetic fluid under the magnetic field were done very extensively [5–18]. It seems that the spatial ordering of magnetic nanoparticles influences the ultrasonic propagation and by analysing this it is possible to understand the structure of magnetic fluids. Recently, the interest has been renewed to understand the structure of magnetic fluid both experimentally and theoretically using acoustic properties [19–30].

DOI: 10.1007/s12043-011-0142-z; *e*Publication: 2 August 2011

In dilute magnetic fluid, concentration of the magnetic particles is sufficiently low; the magnetic grains interact with the external magnetic field but do not interact with each other. This is true if the coupling constant $\lambda = \mu^2/d_h^3 kT$ (a measure of dipolar strength) of the neighbouring grain is much smaller [31]. Here μ is the magnetic moment of the grain, d_h is the hydrodynamic diameter of the grain, k is the Boltzmann constant and T is the absolute temperature. But for higher concentration and high magnetic field, it stimulates the formation of chain/clusters and rigidity of the ferrofluid increases. This affects the propagation of ultrasound wave in the medium.

In 1975, Parson [7] proposed linear hydrodynamic theory of the magnetic fluid under a magnetic field and derived an expression for sound attenuation coefficient. He showed the dependence of velocity and attenuation on the angle between sound wave vector and external magnetic field. This behaviour can be explained using $\sin^2 2\theta$ dependence. The existence of such anisotropic behaviour was confirmed experimentally by Chung and Isler [8,9,11], but they have observed a deviation from $\sin^2 2\theta$ behaviour. Gotoh *et al* [10], however, have derived the expression for the attenuation coefficient using ferrohydrodynamics theory. Later, Tarapov *et al* [5,6,13] have derived an expression for perturbation velocity using thermodynamic state equation and assuming a magnetic liquid as a non-homogenously and isotropically magnetized medium. Using this they have explained quantitatively the experimental results of Chung and Isler [8]. Considering chain-like cluster formation and rotational and translation motions of the magnetic particles, Takatomi [14] has derived the expression for attenuation coefficient. This model seems to explain qualitatively the experimental findings [16]. Recently, Shliomis *et al* [29] have shown the absorption of acoustic energy by internal degree of freedom of short chains as a new viable mechanism of ultrasound attenuation in magnetic fields. They have also verified their model with the experimental findings of Jozefezak *et al* [26]. In addition, they have demonstrated that even though the volume fraction of the chains may be quite small, such an effect may reach the order of magnitude of viscous damping.

In this study, we measure change in ultrasonic propagation velocity, $\Delta V/V_{H=0}$, in a hydrocarbon-based $Mn_{0.7}Zn_{0.3}Fe_2O_4$ magnetic fluid for varying temperature and field at 2 MHz frequency. The choice of the method is based on the earlier findings by Chung and Isler [8,9], where they have shown that pulse-echo experiments are suitable for attenuation studies whereas continuous wave method is suitable for studying the velocity change due to the magnetic field. The direction of ultrasonic wave propagation is perpendicular to the direction of magnetic field. We have to mention that, extensive studies have been carried out to understand the effect of magnetic field on ultrasonic velocity propagation for $\theta = 0°$, but very few experimental studies are reported for 90°. Results of our investigation show that considering the moment distribution of magnetic particles and Tarapov's theory [13], it is possible to explain the observed behaviour in velocity anisotropy of ultrasound in fluid for a perpendicular configuration. This can be explained by assuming grain–grain interaction.

2. Experimental procedure

2.1 *Magnetic fluid synthesis*

$Mn_{0.7}Zn_{0.3}Fe_2O_4$ nanoparticles were synthesized by co-precipitation technique followed by digestion. Analytical grade reagents of ferric, manganese and zinc chloride were mixed in

an appropriate ratio to get a solution containing Fe^{3+}, Zn^{2+} and Mn^{2+} ions. By adding 8 M NaOH solution at 300 K ferrite particles were precipitated which were digested at 90°C for 30 min. During this time, the particles grew and transformed to the crystalline state. Oleic acid was then added to the mixture and stirred for an hour. The fluid was heated at 92°C for 5 min and peptized by adding dilute HCl. The oleic acid-coated particles were washed repeatedly with double-distilled water and separated by magnetic sedimentation. Finally, the coated particles were washed with acetone to remove the water. This acetone wet slurry was dispersed in kerosene, and acetone was removed by heating. This kerosene-based fluid is stable with time.

X-ray diffraction pattern of $Mn_{0.7}Zn_{0.3}Fe_2O_4$ nanoparticles is shown in figure 1. The pattern reveals the formation of single-phase fcc spinel structure. Detailed analysis of the pattern has been carried out using a Rietveld refinement program [32]. In figure 1 solid line shows Rietveld refined fit of the experimental data (open symbol). The relevant parameters derived from the fit are: lattice parameter: 0.846 ± 0.001 nm, oxygen parameter: 0.0261 ± 0.0001, particle diameter: 9.7 ± 0.5 nm.

2.2 *Magnetic characterization*

The room temperature (300 K) magnetization of $Mn_{0.7}Zn_{0.3}Fe_2O_4$ nanomagnetic fluid as a function of magnetic field (B) is shown in figure 2. It exhibits superparamagnetic nature at a given temperature. In the nanoparticle system, to analyse the data, one considers size or moment distribution as volume distributions are ubiquitous. In ideal superparamagnetic systems, μ is proportional to volume and the moment distribution arises only due to a

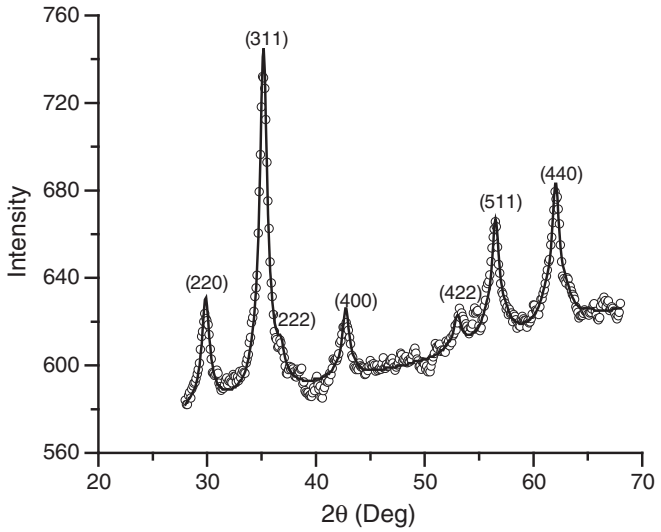

Figure 1. Powder X-ray diffraction profile of the dried $Mn_{0.7}Zn_{0.3}Fe_2O_4$ ferrofluid sample. The solid line through the data points are Rietveld fit. The best fit parameters are: lattice constant: 0.846 ± 0.001 nm, oxygen parameter: 0.026 ± 0.001, particle diameter: 9.7 ± 1 nm. χ^2 value is 1.89.

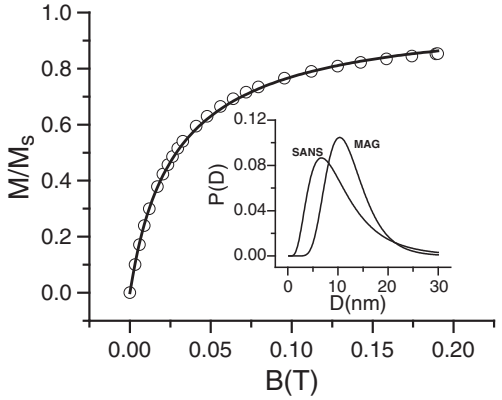

Figure 2. The room temperature (300 K) magnetization curve for Mn–Zn fluid sample. The line shows the best fit to eq. (1) after incorporating the moment distribution function given by eq. (2). The fit parameters are: $\mu_0 = 2.6 \times 10^{-19}\text{Am}^2$ and $\sigma = 1.04$. Inset: Size distribution obtained from SANS and magnetization.

volume distribution. However, in real systems, surface disorder, frustration and spin canting may contribute to moment distribution unlike the volume distribution. Therefore, in this work we have analysed the magnetization curve by considering moment distribution, with the total magnetization expressed as

$$M(B,T) = n\int_{\mu_{\min}}^{\mu_{\max}} \mu L(\xi) f(\mu)\,\mathrm{d}\mu, \tag{1}$$

where

$$L(\xi) = \coth\xi - 1/\xi,$$
$$\xi = \mu B/kT.$$

n is the number density of the particle, μ is the particle moment and $f(\mu)$ is the normalized moment distribution expressed by

$$f(\mu) = \frac{1}{\mu\sigma\sqrt{2\pi}} \exp\left[-\left\{\frac{\ln(\mu/\mu_0)^2}{2\sigma^2}\right\}\right]. \tag{2}$$

The mean particle moment $\langle\mu\rangle$ is equal to $\mu_0 \exp(\sigma^2/2)$, where σ^2 is the variance of the normally distributed $\ln(\mu)$. In figure 2 the fit to eqs (1) and (2) is shown by a solid line. The experimental data match well with theory, and the parameters obtained are: $\mu_0 = 2.6 \times 10^{-19}\text{Am}^2$ and $\sigma = 1.04$. If one considers that the mean particle magnetic moment is proportional to the volume (i.e $\langle\mu\rangle = M_\mathrm{d} * V$, where V is the volume of the particle); considering the domain magnetization (M_d) of the particle as 320 kA/m (obtained from magnetization measurements), the mean particle diameter $\langle D\rangle$ is 13.9 nm and $\sigma(D) = \sigma(\mu)/3 = 0.35$. This observed value of size is higher than that obtained from SANS (small angle neutron scattering) (inset of figure 2) [33] and X-ray. This deviation can be due to grain–grain interaction, as dipolar interaction among particles introduces a self-averaging effect over the correlation length, which results in larger average 'magnetic' size of the apparent particles together with a narrower size distribution.

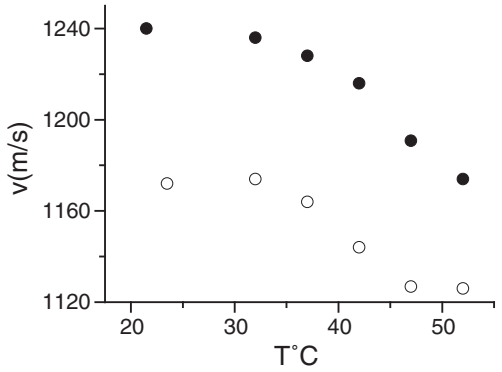

Figure 3. Temperature dependence of ultrasonic propagation velocity of (•) carrier fluid and (○) magnetic fluid.

2.3 *Measurement of ultrasonic propagation velocity*

To study the frequency dispersion in magnetic fluids, we have used a multi-frequency ultrasonic interferometer (Model M-82, Mittal Enterprises, India) operating in the range 1–10 MHz. The multi-frequency generator generates very stable continuous ultrasonic waves (±0.03%) in the given range. The desired frequency was selected and the signal was then fed through a coaxial cable to the measuring cells. Each cell was provided with a quartz crystal whose resonant frequency coincided with that of the signal. The velocity could be measured with an accuracy of ±0.3%. To measure the velocity at different magnetic fields the measuring cell was placed in an electromagnet having a pole gap of 2 inch. The maximum field strength of the electromagnet was 0.1 T. The angle (θ) between the magnetic field direction and the direction of ultrasonic wave propagation was 90°.

Figure 3 shows the temperature dependence of ultrasonic velocity of the carrier and the magnetic fluid at 2 MHz frequency. The velocity of the fluid is 7% lower than that of the carrier liquid in the absence of magnetic field, which shows the influence of dispersed particles on the ultrasonic propagation velocity. The velocity profile of the carrier fluid and the magnetic fluid with temperature is nearly similar indicating the minimal influence on the ultrasonic propagation velocity.

3. Results and discussion

3.1 *Magnetic field dependence*

Figure 4 shows the magnetic field dependence of ultrasonic propagation velocity anisotropy, $\Delta V/V_{H=0}$, at 308 K. In this experiment, the magnetic field was applied, and data were recorded after 20 min. This procedure was repeated for each field. From figure 4 it is observed that the magnitude of $\Delta V/V_{H=0}$ decreases initially with field, reaches a minimum, and thereafter it increases. At a higher field, it exhibits saturation behaviour. This is similar to the observations by Chung *et al* [7,8].

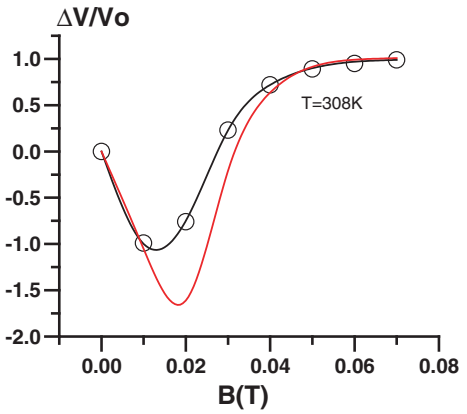

Figure 4. Anisotropy in velocity at 2 MHz with magnetic field at 308 K. The dotted line is best fit to Tarapov's theory [13] for $\mu_0 = 3.2 \pm 0.02 \times 10^{-19}\mathrm{Am}^2$. The solid line is fit to Tarapov's theory after incorporating polydispersity in the magnetic moment. The fit values are: $\mu_0 = 3.02 \pm 0.02 \times 10^{-19}\mathrm{Am}^2$ and $\sigma = 0.33$ (see text).

In magnetic fluids, sound waves are coupled to the magnetic variables as the magnetization oscillates with fluid density. Tarapov *et al* [13] have derived the equation for the sound wave propagation in magnetic fluid, based on hydrodynamical equations of motions. It is known that in the absence of magnetic field the fluid is being treated as homogeneous and isotropic, but under the influence of the field, due to aggregation and restructuring of dispersed particles, fluid becomes inhomogeneous and anisotropic. The degree of inhomogeneity depends on volume fraction, field strength, temperature and other such factors. These factors influence magnetic as well as thermodynamic properties of the magnetic fluids. Considering the propagation of weak oscillations in such a fluid with the wavelength much greater than aggregate size, their effect on anisotropy can be neglected and the ferrofluids can be considered as inhomogeneous and isotropically magnetized media. Nevertheless, based on this argument, Tarapov *et al* [13] have derived the equation for velocity of weak perturbation propagation.

According to [13], the change in ultrasonic propagation velocity is given by

$$\left(\frac{\Delta V}{V_0}\right)\% = L_0 - \frac{L_1 \sin^2\theta}{\left(1 + L_2 \sin^2\theta\right)}. \tag{3}$$

For $\theta = 90°$, the variation of velocity anisotropy with field for $\mu_0 = 3 \times 10^{-19}\,\mathrm{Am}^2$ is calculated and the contribution of each term A and B (terms A and B are the first and second terms of eq. (3), respectively) along with the resultant curve is shown in figure 5. It is evident from figure 5 that by increasing field the first term A saturates at about 0.0175 T and at same time B starts decreasing. The variation of velocity anisotropy for different values of μ_0 is shown in figure 6. It is clear from figure 6 that as the moment increases (i.e. increase in size and/or domain magnetization of the particle) the contribution of B increases faster compared to A which result in a net decrease in velocity anisotropy. The inset of figure 6 shows the modulus of velocity anisotropy for $\mu_0 = 2 \times 10^{-19}\mathrm{Am}^2$. The observed behaviour is similar to that obtained by Chung and Isler [8]. In figure 4,

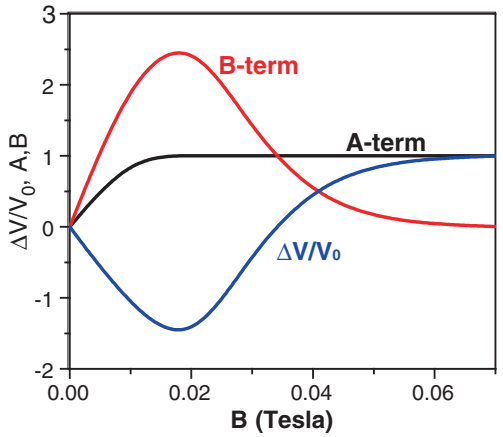

Figure 5. Contribution of each term A and B of Tarapov's theory (eq. (3)) along with the resultant graph for $\mu_0 = 3 \times 10^{-19}\mathrm{Am}^2$ (see text).

the fit generated using $\mu_0 = 3.2 \times 10^{-19}\mathrm{Am}^2$ is shown as red line. The fit is not good at intermediate fields. The value of particle diameter corresponding to this value of μ_0 is 12.4 nm.

In eq. (3), the parameters L_0, L_1 and L_2 are functions of magnetization, field and temperature. The magnetic particles dispersed in the magnetic fluids are not mono-dispersed, thus one needs to account for the polydispersity in the moment. Figures 7a and 7b, show respectively, the effect of μ_0 and σ on the velocity anisotropy generated using eqs (1) and

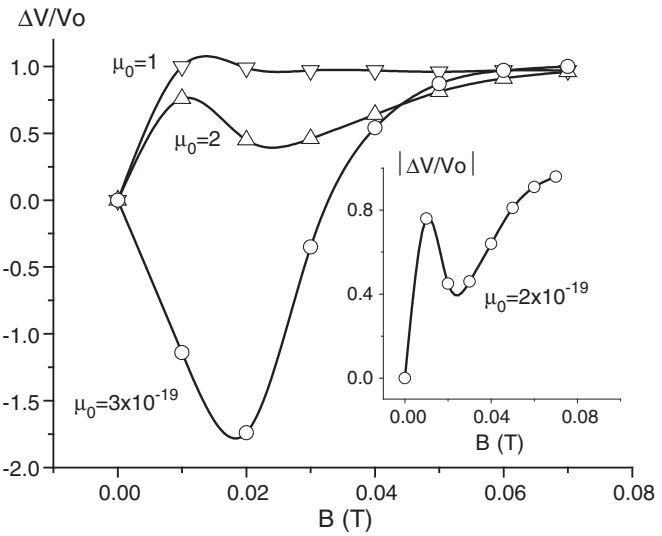

Figure 6. Anisotropy of ultrasonic velocity for $\theta = 90°$ and for different values of μ_0 calculated using eq. (3) at 308 K. Inset: $|\Delta V/V_0|$ with field for $\mu_0 = 2 \times 10^{-19}\mathrm{Am}^2$. The behaviour is similar to that obtained in ref. [8].

(3). The following conclusions can be drawn from figure 7. By increasing the moment distribution, the minimum first shifts towards the lower field and then decreases in magnitude (figure 7a). This change in magnitude is higher when the moment is reduced (figure 7b). Thus the moment and its distribution do influence the behaviour of velocity anisotropy. To get better fit to the observed experimental result, we have introduced the moment distribution function (eq. (1)) and recalculated. The solid line in figure 4 is the line generated for $\mu_0 = 3.05 \pm 0.02 \times 10^{-19}\text{Am}^2$ and $\sigma = 0.32 \pm 0.01$. This corresponds to the mean diameter $\langle D \rangle = 12.5$ nm and $\sigma(D) = 0.1$. The observed narrow size distribution indicates the influence of the interparticle interaction in the system.

3.2 *Temperature dependence*

In steric stabilized magnetic fluid, the forces responsible for stability are long-range van-der Waals's interaction, steric interaction and dipole–dipole interaction. The first two are isotropic in nature whereas the third is anisotropic (i.e. directional) in nature. The magnetic dipole–dipole interaction profile is the same whether particles are dispersed in an aqueous or non-aqueous carrier, but van-der Waals's interaction profile differs considerably. In a non-aqueous carrier, the surfactants are essentially indistinguishable from the solvent, and therefore, their contribution to overall van-der Waals's interaction is negligible. Thus the only interaction which contributes to total interaction energy is the dipole–dipole interaction, which favours chain formation, the magnitude of which is of the order of 1–2kT. This means that they are susceptible to thermal force.

In view of the above we have studied the temperature dependence of ultrasonic propagation under different magnetic fields. Figure 8 shows the effect of temperature on the velocity anisotropy. The following observations are drawn from figure 8: (i) The anisotropy minimum shifts towards the lower field as the temperature is increased, and the minimum gets broader, (ii) the sign of $\Delta V/V_{H=0}$ changes at 42°C. When

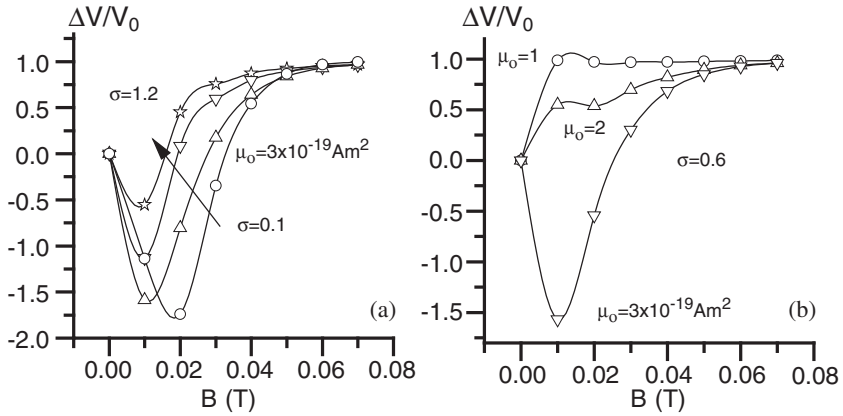

Figure 7. Influence of moment distribution on anisotropy velocity calculated using eqs (2) and (3) for (**a**) different values of σ when $\mu_0 = 3 \times 10^{-19}\text{Am}^2$, (**b**) different values of μ_0 when $\sigma = 0.6$.

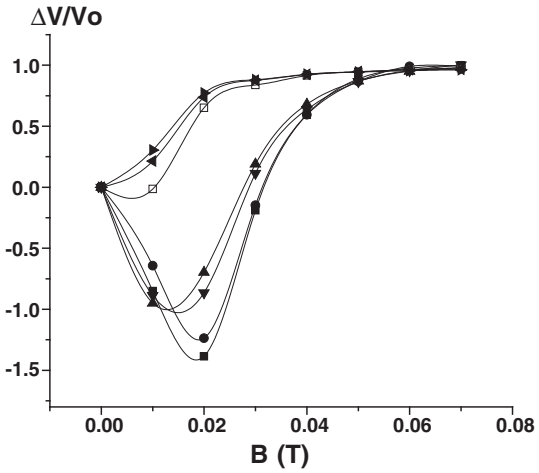

Figure 8. Temperature dependence of velocity anisotropy. (■) 22°C, (●) 32°C, (▼) 35°C, (▲) 37°C, (□) 42°C, (◄) 47°C, (►) 52°C. The line is fit to eqs (2) and (3). With increasing temperature the moment distribution becomes broader, indicating the decrease in grain–grain interaction.

all these data were fitted using eqs (1) and (3), it is observed that μ_0 remains constant $\left(\mu_0 = 3.05 \pm 0.02 \times 10^{-19}\mathrm{Am}^2\right)$ but σ increases with temperature from 0.1 to 1.67 (figure 9). This corresponds to the variation of effective mean particle diameter from 12.4 nm to 19.1 nm. This indicates that with an increase in temperature mean diameter increases 1.6 times but the size distribution becomes 16 times broader. This is understandable because with an increase in thermal energy randomizing Brownian energy increases, which reduces the magnitude of the anisotropy and broadens the minimum. Thus, in the

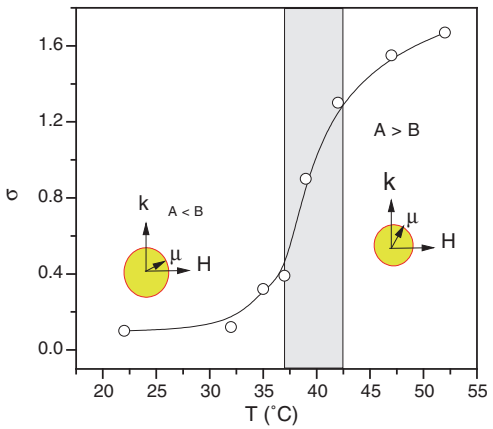

Figure 9. Variation in size distribution with temperature obtained from figure 8. The orientation of the cluster/particle moment, with respect to the magnetic field, below and above the critical temperature region (shaded area) is also shown.

present system, the change in velocity anisotropy is dominated by grain–grain interaction rather than grain–field interaction.

4. Conclusion

The magnetic field-induced ultrasonic velocity anisotropy (for $\theta = 90°$) in $Mn_{0.7}Zn_{0.3}Fe_2O_4$ magnetic fluid was studied as a function of temperature. It is reported that variation in velocity anisotropy at a given temperature depends on the value of the magnetic moment and the size distribution. The observed behaviour is explained by incorporating the moment distribution function in Tarapov's theory. The study reveals that the anisotropy is dominated by grain–grain interaction and the magnitude of this interaction decreases with increasing temperature.

Acknowledgement

The work is carried out under Gujarat Science & Technology (GUJCOST), Govt. of Gujarat, India.

References

[1] S Odenbach, *Magnetoviscous effects in ferrofluids, Lecture Notes in Physics* (Springer, Berlin, 2002) Vol. 71
[2] S Thurm and S Odenbach, *Phys. Fluids* **15**, 1658 (2003)
[3] M Kroger, P Ilg and S Hess, *J. Phys. Condens. Matter* **15**, S1403 (2003)
[4] P Ilg, M Kroger and S Hess, *Phys. Rev.* **E71**, 031205 (2005); **72**, 031504 (2005)
[5] I Ye Tarapov, *Magnitin. Gidrodinamika* **1**, 3 (1972)
[6] I Ye Tarapov, *Prikl. Mat. Mekh.* **37**, 813 (1973)
[7] J D Parson, *J. Phys. D: Appl. Phys.* **8**, 214 (1975)
[8] D Y Chung and W E Isler, *J. Appl. Phys.* **49**, 1809 (1978)
[9] W E Isler and D Y Chung, *J. Appl. Phys.* **49**, 1812 (1978)
[10] K Gotoh, W E Isler and D Y Chung, *IEEE Trans. Magn. MAG-2*, **211–213** (1980)
[11] D Y Chung, H Z Hung and J X Lin, *J. Magn. Magn. Mater.* **39**, 111 (1983)
[12] S P Vaidya and R V Mehta, *J. Magn. Magn. Mater.* **39**, 82 (1983)
[13] I Ye Tarapov, N F Patsegon and A I Phedonenko, *J. Magn. Magn. Mater.* **39**, 51 (1983)
[14] S Taketomi, *J. Phys. Soc. Jpn.* **55**, 838 (1986)
[15] R V Mehta and J M Patel, *J. Magn. Magn. Mater.* **65**, 204 (1987)
[16] R Shrivastava, S P Vaidya, J M Patel and R V Mehta, *J. Colloid Interface Sci.* **124**, 248 (1988)
[17] V V Gogosov, A V Gorbunov, S N Tsurikov, A A Usanov and A N Vinogradov, *J. Magn. Magn. Mater.* **122**, 70 (1993)
[18] K Henje, *Phys. Rev.* **E50**, 1184 (1994)
[19] A Skumiel, T Hornowki and M Labowski, *Ultrasonics* **36**, 421 (1998)
[20] T Sawada, H Nishiyama and T Tabata, *J. Magn. Magn. Mater.* **252**, 186 (2002)
[21] M Motozawa and T Sawada, *Proceeding of 3rd Int. Symposium on Ultrasonic Doppler Methods for Fluid Mechanics and Fluid Engineering* (EPFL, Lausanne, Sept. 9–11, 2002) p. 137
[22] T Hornowski, A Jozefczak, M Labowski and A Skumiel, *Mol. Quantum Acoustics* **24**, 31 (2003)

[23] A Skumiel, A Jozefczak, T Hornowski and M Labowski, *J. Phys. D: Appl. Phys.* **36**, 3120 (2003)
[24] M Motozawa, Y Matsmoto and T Sawada, *JSME Int. J. Ser.* **B48**, 471 (2005)
[25] M Motozawa and T Sawada, *J. Magn. Magn. Mater.* **289**, 66 (2005)
[26] A Jozefczak and A Skumiel, *J. Phys.: Condens. Matter* **18**, 1869 (2006)
[27] B S Ebinezer and L Palaniappan, *J. Phys. Sci.* **18**, 1 (2007)
[28] M Motozawa, Y Iizuka and T Sawada, *J. Phys.: Condens. Matter* **20**, 204117 (2008)
[29] M Shliomis, M Mond and K Morozov, *Phys. Rev. Lett.* **101**, 074505 (2008)
[30] M A Bramantya, M Motozawa, H Takuma and T Sawada, *J. Phys: Conf. Ser.* **149**, 012040 (2009)
[31] R E Rosensweig, *Ferrohydrodynamics* (Cambridge University Press, Cambridge, 1985)
[32] The Rietveld Refinement Program–DBWS–9006PC, developed by Dr H Marciniat, Poland, for X-ray powder and neutron powder diffraction data
[33] V K Aswal and P S Goyal, *Curr. Sci. India* **79**, 947 (2000)